

A Theoretical and Practical Framework for Evaluating Uncertainty Calibration in Object Detection

P. Conde, R. L. Lopes, C. Premebida

Abstract—The proliferation of Deep Neural Networks has resulted in machine learning systems becoming increasingly more present in various real-world applications. Consequently, there is a growing demand for highly reliable models in these domains, making the problem of uncertainty calibration pivotal, when considering the future of deep learning. This is especially true when considering object detection systems, that are commonly present in safety-critical application such as autonomous driving and robotics. For this reason, this work presents a novel theoretical and practical framework to evaluate object detection systems in the context of uncertainty calibration. The robustness of the proposed uncertainty calibration metrics is shown through a series of representative experiments.

Index Terms—Uncertainty Calibration, Object Detection, Reliability, Global Calibration, Local Calibration.

I. INTRODUCTION

Deep Neural Networks (DNNs) have revolutionized the applicability of Machine Learning (ML) systems in real-world scenarios. These powerful Deep Learning (DL) models are now extensively used in critical domains such as autonomous driving, medicine, remote sensing, and robotics, where the consequences of erroneous decisions can be severe. Consequently, it is vital for DNNs to provide reliable confidence scores that accurately quantify the uncertainty associated with their predictions. For this reason, the problem of uncertainty calibration (also called *confidence calibration* or simply *calibration*) is becoming ubiquitous when developing DL models that are reliable and robust enough for real-world applicability.

The importance of uncertainty calibration of DNNs is illustrated by the growing body of scientific work, developed in recent years regarding this subject [2], [8], [13], [15]. Nonetheless, most of these works are developed around the problem of uncertainty calibration in classification problems. Contrastingly, a lot of DL safety-critical applications are related to object detection problems (*e.g.*, autonomous driving, robotics, surveillance, tracking). We argue that one of the main reasons for a lack of scientific work regarding uncertainty calibration in object detection scenarios is due to the fact that there is no complete/proper theoretical and practical formulation regarding the understanding and evaluation of this

problem. As such, the work here developed aims at filling this gap found in relevant scientific literature. Therefore, the key contributions of this work are twofold:

- A proper theoretical formulation of the uncertainty calibration problem in object detection (Section III) that, to the best of our knowledge, is absent in relevant literature.
- Three novel uncertainty calibration metrics ¹ specifically designed for the context of object detection evaluation (Section IV), consistent with the above mentioned theoretical formulation.

II. RELATED WORK

The problem of uncertainty calibration is introduced to the DL community through the work presented in [4], where the calibration quality of various modern DNNs is evaluated on classification problems, with distinct datasets, from computer vision and natural language processing domains. The authors argue that despite their increased accuracy, modern DNNs suffer from significant miscalibration issues, which surpass those observed in ‘older’ but less accurate architectures.

The evaluation of uncertainty calibration in classification problems often relies on the widely used Expected Calibration Error (ECE) [11]. However, limitations of this metric have been acknowledged in relevant literature [12], [16]. On the other hand, the use of *proper scoring rules* [3] like the Brier score [1] has been an increasingly common practice in recent literature regarding uncertainty calibration for classification problems [8], [13], [15].

The lack of evaluation metrics specifically designed to the problem of uncertainty calibration in object detection is addressed in [6], that proposes the Detection Expected Calibration Error (D-ECE). Since then, this metric has been adopted as a “go-to” evaluation metric in different works regarding uncertainty calibration in object detection [9], [10], [14]. Nonetheless, the D-ECE is built on an incomplete formulation of the problem of uncertainty calibration in object detection, and therefore does not incorporate the effect of False Negative detections (see Section IV for further details).

III. UNCERTAINTY CALIBRATION FOR OBJECT DETECTION

In this section we formally introduce the concept of uncertainty calibration, when considering object detection scenarios.

¹Code for the proposed uncertainty calibration metrics at: https://github.com/pedromconde/Uncertainty_Calibration_Object_Detection.

The presented definitions are largely inspired in the concept of uncertainty calibration for classification problems [16], though adapted to the particularities of the object detection's case.

For the subsequent definitions we will consider \mathcal{X} , the sample space of inputs, $(\mathcal{Y}, \mathcal{K})$ the sample space of bounding-box locations, and respective classes. We can now consider the respective random variables, X and (Y, K) , defined under those sample spaces. Let us note that a realization of (Y, K) can define an arbitrary number of locations (bounded by the total number of possible locations) and respective classes *i.e.*, any realization of (Y, K) , for a problem with C different classes, is a subset of $\Omega \times \{1, \dots, C\}$, where $\Omega \subset \mathbb{N}^4$. For this reason, we will denote as $P((y, c) \in (Y, K))$ the abbreviation of $P(\{\vartheta, \psi \in (\mathcal{Y}, \mathcal{K}) : y \in Y(\vartheta) \wedge c \in K(\psi)\})$ *i.e.*, the probability that some singular bounding-box location (with respective class) belongs to some realization of (Y, K) .

Before considering the concept of calibration in the context of object detection, we must primarily define the mathematical object for which such considerations are pertinent *i.e.*, a **probabilistic detector**. Let us first consider the function $\Psi : \mathcal{X} \rightarrow (\mathcal{Y}, \mathcal{K})$, that maps an input from the sample space \mathcal{X} to the set of all possible bounding-box locations in that specific input. We are now in conditions to assert the following definition.

Definition 1: We define a **probabilistic detector** (for a problem with C classes) as a function $f : \mathcal{X} \rightarrow \Phi$, that maps each input to a set of all possible bounding-box locations and correspondent confidence scores, for each respective class. Formally, $\forall x \in \mathcal{X}$, we have that

1. $f(x) \subseteq \Omega \times \{1, \dots, C\} \times [0, 1]$ (1)
2. $(l, c) \in \Psi(x) \iff (l, c, p) \in f(x)$. (2)

Although in a practical scenario most object detection systems will not consider all possible bounding-box locations, from a theoretical point-of-view this is a reasonable definition, because we can associate all disregarded locations with a confidence score equal to 0. We note that $(l, c, p) \in f(x)$ denotes a bounding-box detections of the form (*Location, Class, Confidence score*).

Let us observe that, since most object detection systems incorporate suppression strategies (like *Non Maximum Suppression*), considering the concept of calibration for pinpoint localization is unreasonable in a practical scenario. As such, let us take as $\mathcal{F} : \Omega \times \Omega \rightarrow [0, 1]$ to designate the well known *Intersection Over Union* (IoU) function, and define (for some threshold value $\tau \in [0, 1]$) $\varphi_\tau : \Omega \times \{1, \dots, C\} \rightarrow [0, 1]$ as

$$\varphi_\tau(y, c) = \max \{p : (l, c, p) \in f(X) \wedge \mathcal{F}(y, l) \geq \tau\}. \quad (3)$$

It is worth observing that, following the definition of a *probabilistic detector* (Definition 1), the value of $\varphi(y, c)$ can be 0 (this is the case were there is no positive prediction that satisfies the condition $\mathcal{F}(y, l) \geq \tau$). We can now consider the following definition

Definition 2: We say that a probabilistic detector $f : \mathcal{X} \rightarrow \Phi$ is **globally calibrated** (for some threshold value $\tau \in [0, 1]$)

iff

$$P((y, c) \in (Y, K) \mid (l, c, p) \in f(X)) = \varphi_\tau(y, c). \quad (4)$$

Based on Definition 2 we will develop new evaluation metrics, constructed with the purpose of assessing the calibration of the predictive uncertainty of probabilistic detectors in a practical object detection scenario.

A weaker formulation of the uncertainty calibration problem in object detection, similar to that used in [6], can also be outlined, by considering only the calibration of the detections that have a positive confidence score associated (*i.e.*, the detections that are actually returned by a model in a practical scenario).

Definition 3: We say that a probabilistic detector $f : \mathcal{X} \rightarrow \Phi$ is **locally calibrated** (for some threshold value $\tau \in [0, 1]$) iff

$$P((y, c) \in (Y, K) \mid (l, c, p) \in f(X), p > 0, \mathcal{F}(y, l) \geq \tau) = \varphi_\tau(y, c). \quad (5)$$

We care to note that such formulation is not sensible to False Negative predictions (see section IV).

IV. EVALUATION METRICS

a) Notation: We define *bag* (also called a *multiset*) as an extension of the notion of *set*, that can have repeated elements (*i.e.*, different instances of the same element).

Evaluating uncertainty calibration, in a practical object detection setting, encompasses some of the same challenges found when evaluating this problem in a classification scenario, regarding the nonexistence of ground-truth information for the true likelihood values (left side of both Equations (4) and (5)). For this reason, and just like in the classical classification setting, emerges the need to develop practical evaluation metrics in relation to the previously outlined formal definitions. Therefore, considering the theoretical formulation presented in Definition 2, we have developed uncertainty calibration evaluation metrics in the context of object detection.

Before introducing such metrics, some definitions have to be made that are common in the context of object detection problems, and will be necessary when evaluating uncertainty calibration. Let us take a probabilistic detector $f : \mathcal{X} \rightarrow \Phi$, a finite set of inputs $\mathcal{X}' \subset \mathcal{X}$, and the bag of respective ground truth locations and classes $(\mathcal{Y}', \mathcal{K}') \subset (\mathcal{Y}, \mathcal{K})$. In a setting of this type, and for some threshold value $\tau \in [0, 1]$, we can define the bags TP_τ , as the bag of confidence scores associated with *True Positives* (detections that have a corresponding ground-truth with an IoU greater than τ), FP_τ , as the bag of confidence scores associated with *False Positives* (detections that do not have a corresponding ground-truth with an IoU greater than τ), and FN_τ , as the bag of confidence scores associated with *False Negatives* (ground-truth bounding boxes with no corresponding detection with an IoU greater than τ). We care to note that, although FN_τ is a bag of identical (theoretically zero-valued) confidence scores, the number of such detections will be fundamental in the computation of the proposed uncertainty calibration metrics.

In the following subsections we propose three novel uncertainty calibration metrics based on Definition 2. The first two metrics (Subsections IV-A and IV-B) are based on proper scoring rules [3], while the third one (Subsection IV-C) relies on bin-wise computations, similarly to the ECE [11].

A. Quadratic Global Calibration Score

Inspired in the Brier score [1] - a proper scoring rule widely used to evaluate uncertainty calibration in classification problems - we introduce in this section the Quadratic Global Calibration (QGC) score, that leverages the same fundamental principle of its predecessor, by computing the quadratic difference between a confidence score and its true response.

We start by considering (as in the previous section) a probabilistic detector $f : \mathcal{X} \rightarrow \Phi$, a finite set of inputs \mathcal{X}' and the bag of respective ground truth locations and classes $(\mathcal{Y}', \mathcal{K}')$. In this context we can construct our bags TP_τ , FP_τ and FN_τ .

The QGC score can now be computed as

$$\text{QGC} = \sum_{p \in \text{TP}_\tau \cup \text{FN}_\tau} (p-1)^2 + \sum_{p \in \text{FP}_\tau} p^2 \quad (6)$$

$$= \sum_{p \in \text{TP}_\tau} (p-1)^2 + \sum_{p \in \text{FP}_\tau} p^2 + |\text{FN}_\tau|. \quad (7)$$

A lower value of QGC score translates a better performance in terms of uncertainty calibration, reaching its optimal value at 0.

B. Spherical Global Calibration Score

The Spherical Global Calibration (SGC) score is inspired in a less common proper scoring rule, the Spherical score [3]. Let us first denote

$$r(p) = \sqrt{p^2 + (1-p)^2}. \quad (8)$$

A direct adaptation of the Spherical score would be formulated as

$$\text{SGC}^* = \sum_{p \in \text{TP}_\tau \cup \text{FN}_\tau} \frac{p}{r(p)} + \sum_{p \in \text{FP}_\tau} \frac{1-p}{r(p)}. \quad (9)$$

Such formulation reaches its optimal value at $N = |\text{TP}_\tau| + |\text{FP}_\tau| + |\text{FN}_\tau|$, while a higher value translates a better performance (similar to the original Spherical score). As such, we define the SGC score as

$$\text{SGC} = \sum_{p \in \text{TP}_\tau \cup \text{FN}_\tau} \left(1 - \frac{p}{r(p)}\right) + \sum_{p \in \text{FP}_\tau} \left(1 - \frac{1-p}{r(p)}\right) \quad (10)$$

$$= N - \sum_{p \in \text{TP}_\tau} \frac{p}{r(p)} - \sum_{p \in \text{FP}_\tau} \frac{1-p}{r(p)}. \quad (11)$$

Now, just like with the QGC score, a lower value of SGC score translates a better performance in terms of uncertainty calibration, reaching its optimal value at 0.

C. Expected Global Calibration Error

The Expected Global Calibration Error (EGCE) is an adaptation of the popular ECE [11]. The ECE is widely used to

evaluate uncertainty calibration in classification problems, that works based on the principle of computing the bin-wise difference between average confidence scores and average accuracy. Since the original ECE leverages the concept of ‘‘accuracy’’ - common in the evaluation of classification systems - the use of the EGCE will require an adaptation of this concept to the context of object detection. In fact, such challenge is also addressed in [6], in the development of the D-ECE. Therefore, EGCE will be largely based on the same principle of the D-ECE, while incorporating the necessary adaptations to address the previously discussed limitations of this metric.

We start by creating the sets of bins $\{B_1^{\text{TP}_\tau}, \dots, B_M^{\text{TP}_\tau}\}$ and $\{B_1^{\text{FP}_\tau}, \dots, B_M^{\text{FP}_\tau}\}$, where each bin is a bag of confidence scores defined as

$$B_i^{\text{TP}_\tau} = \{p \in \text{TP}_\tau : p \in](i-1)/M, i/M]\}, \quad (12)$$

$$B_i^{\text{FP}_\tau} = \{p \in \text{FP}_\tau : p \in](i-1)/M, i/M]\}, \quad (13)$$

for $i = 1, \dots, M$. Additionally, we can now consider the set of bins $\{B_1, \dots, B_M\}$ where each bin is a bag defined as

$$B_i = B_i^{\text{TP}_\tau} \cup B_i^{\text{FP}_\tau}, \quad (14)$$

for $i = 1, \dots, M$. For each bin, we define the average confidence as

$$\text{conf}(B_i) = \frac{1}{|B_i|} \sum_{p \in B_i} p. \quad (15)$$

We will also define the precision per bin as

$$\text{prec}(B_i) = \frac{|B_i^{\text{TP}_\tau}|}{|B_i^{\text{TP}_\tau}| + |B_i^{\text{FP}_\tau}|}. \quad (16)$$

We can now outline the definition of the D-ECE as

$$\text{D-ECE} = \sum_{i=1}^M |B_i| |\text{prec}(B_i) - \text{conf}(B_i)|. \quad (17)$$

Note: in fact, the definition given in [6] is the average of (17) *i.e.*, divided by $|\text{TP}_\tau \cup \text{FP}_\tau|$. Since the D-ECE incorporates only the calibration of the detections that have a positive confidence score associated (*i.e.*, the bags TP_τ and FP_τ), it can be considered a metric for *local calibration* (Definition 3).

The EGCE will leverage a similar principle of the D-ECE by contrasting *precision* and *confidence*. Nonetheless, contrarily to the latter, the EGCE will incorporate False Negative detections, by considering them analogous to False Positives with a confidence of 1, and therefore being incorporated in the last bin. As such, let us then start by considering

$$\delta(B_i) = \frac{|B_i^{\text{TP}_\tau}|}{|B_i^{\text{TP}_\tau}| + |B_i^{\text{FP}_\tau}| + |\text{FN}_\tau|} \quad (18)$$

We can now finally define the EGCE as

$$\begin{aligned} \text{EGCE} = & \sum_{i=1}^{M-1} |B_i| |\text{prec}(B_i) - \text{conf}(B_i)| \\ & + |B_M| |\delta(B_M) - \text{conf}(B_M)|. \end{aligned} \quad (19)$$

Following the same principle as in [6], we will only consider predictions above a given threshold (in our case 0.1), when

	mAP \uparrow	QGC \downarrow	SGC \downarrow	EGCE \downarrow	D-ECE \downarrow
YOLOv5 (Nano)	0.44	23952.82	24882.37	21373.61	3626.55
YOLOv5 (Small)	0.53	20950.61	21857.65	17188.79	2883.91
YOLOv5 (Medium)	0.65	18477.24	19390.43	13461.12	2194.51
YOLOv5 (Large)	0.67	17578.47	18490.01	11831.19	1624.24
YOLOv5 (Extra Large)	0.69	17085.51	17987.22	11100.42	1305.86

TABLE I: Comparing the performance of five different variations of the YOLOv5 [5] object detector, evaluated with mAP, QGC score, SGC score, EGCE and D-ECE, using an IoU threshold of 0.5.

constructing the bags TP_τ , FP_τ and FN_τ for calculating the D-ECE and EGCE (this avoids a bias to the behaviour of low-confidence detections, that is common in this type of bin-wise metrics). Just like the previously proposed metrics, both the D-ECE and the EGCE represent a better performance (in terms of uncertainty calibrations) with lower values, reaching their optimal value at 0. The common number of bins for these types of metrics is between 10 and 20 bins (in our experiments we will use 15 bins).

V. EXPERIMENTS

All the experiments described hereafter are done with pre-trained YOLOv5 [5] object detectors (these models are pre-trained in the training set of the COCO dataset) and evaluated with the COCO validation set of 5000 images [7] (since the official test set has no available ground-truth).

In Table 1 we present the comparison between different versions of the YOLOv5 object detector, namely *Nano*, *Small*, *Medium*, *Large* and *Extra Large*, respectively with 3.2, 12.6, 35.7, 76.8 and 140.7, million parameters. These models are evaluated using the three proposed novel metrics (QGC score, SGC score and EGCE), the D-ECE and also the common *Mean Average Precision* (mAP), using a IoU threshold of 0.5 ($\tau = 0.5$). For this comparison, we present the values of the uncertainty calibration-related metrics with absolute values (instead of the average ones) because, unlike what happens in classification problems (where is common to present the averaged values), different object detection models can output a different number of detections. As such, averaging could create problems when comparing the performance of different models; for example, a model that outputs a large number of low-confidence False Positive detections could appear to perform better in terms of uncertainty calibration than a model with a relatively lower number of False Positive predictions, because of proportionality issues.

Figures 1, 2, 3, 4, 5 and 6 portrait a series of experiments, in which we are interested in evaluating how different types of detections proportionally influence the previously referred four uncertainty calibration metrics (QGC score, SGC score, EGCE and D-ECE). For instance, in Figure 1 we gradually increase the number of False Positive predictions, with confidence scores extracted from a Uniform distribution in the interval $[0.8,1]$; for example, an *increase* of 60% means that it has been added a number of such predictions equal to 60% of the original number of predictions (*i.e.*,

$0.6 \times (|TP_\tau| + |FP_\tau| + |FN_\tau|)$). Specifically, we make such type of experiments with low-confidence and high-confidence False Positives (Figures 1 and 3), low-confidence and high-confidence True Positives (Figures 2, 4 and 5), and also only False Negative detections (Figure 6). In all these experiments, the “starting point” model is the YOLOv5 (Large). The experiments are made starting with a 5% increase, until a 100% increase, with a step of 5%. In the presented results, the values of the previously referred metrics are averaged (contrarily to when we were comparing different models), because in this situation we are actually interested in analysing how specific types of detections proportionally influence the uncertainty calibration metrics. Once again the IoU threshold is set at 0.5.

VI. RESULTS AND DISCUSSION

We start the discussion of the results by analysing Table I. The main conclusions, in a nutshell, are the following: the *Extra Large* version of YOLOv5 performs better in all evaluated metrics; all metrics gradually improve with larger models; EGCE and D-ECE have, proportionally, the biggest differences across the different evaluated models. Finally, we care to note that it is expectable to have an absolute value of the D-ECE smaller than the values of the QGC score, the SGC score and the EGCE, since this metric does not incorporate False Negative detections.

In the remaining of this section, we will focus on the results regarding the connected scatter plots, presented in Figures 1, 2, 3, 4, 5 and 6. It is important to start by observing that, in the context of uncertainty calibration for object detection, it is desirable to have evaluation metrics that penalise both overconfident and underconfident detections, specifically overconfident False Positives (Figure 1), underconfident True Positives (Figure 2) and also False Negatives (Figure 6). On the other hand, our metrics can be expected to reward higher proportions of high-confidence True Positives (Figures 4 and 5), or even low-confidence False Positives (Figure 3).

We start by comparing the behaviour of the proper scoring rule-based metrics, QGC score and SGC score. Our first observation in this regard is that such metrics present a similar behaviour in most cases. Specifically, in Figures 4, 3, 5 and 6, their behaviour is illustrated as nearly identical. In Figures 1 and 2, although still similar, we observe that the SGC score presents a more sensitive behaviour (reflected by stronger increase in value) than the QGC score.

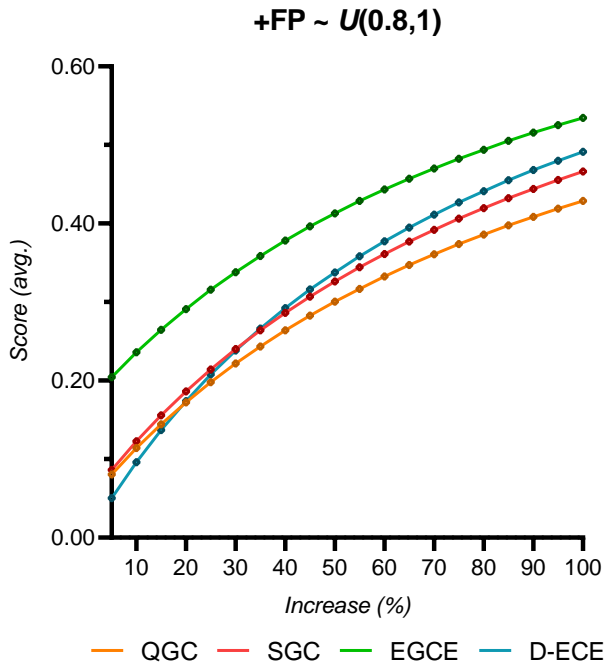


Fig. 1: Evaluating QGC score, SGC score, EGCE and D-ECE, with increasing proportions of False Positive detections, with confidence scores extracted from a Uniform distribution in the interval $[0.8,1]$.

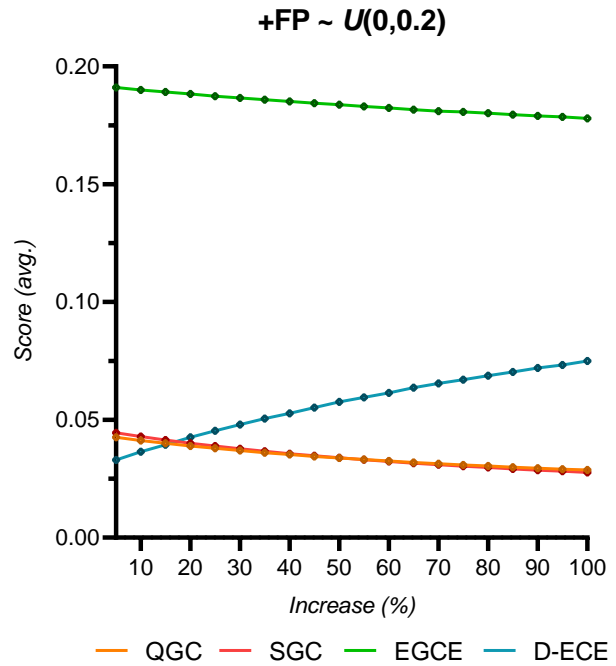


Fig. 3: Evaluating QGC score, SGC score, EGCE and D-ECE, with increasing proportions of False Positive detections, with confidence scores extracted from a Uniform distribution in the interval $[0,0.2]$.

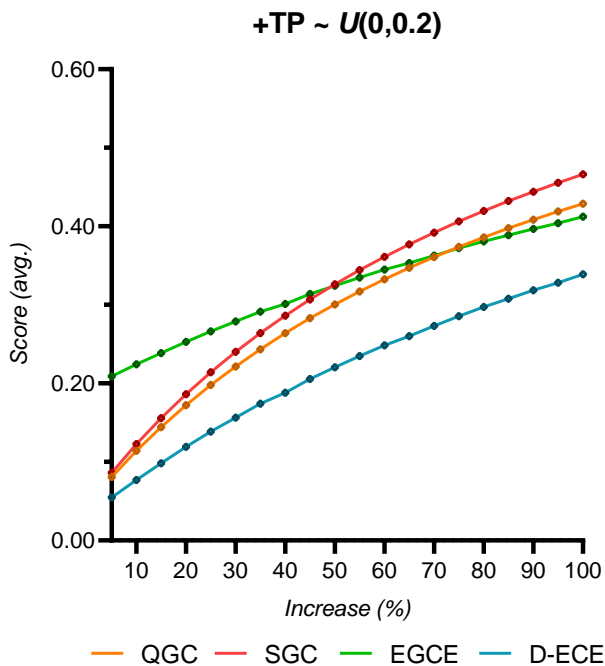


Fig. 2: Evaluating QGC score, SGC score, EGCE and D-ECE, with increasing proportions of True Positive detections, with confidence scores extracted from a Uniform distribution in the interval $[0,0.2]$.

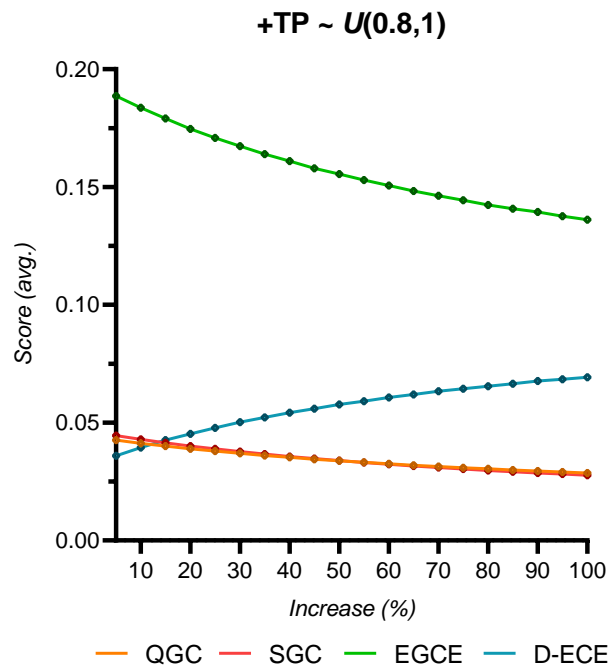


Fig. 4: Evaluating QGC score, SGC score, EGCE and D-ECE, with increasing proportions of True Positive detections, with confidence scores extracted from a Uniform distribution in the interval $[0.8,1]$.

We can now compare the behaviour of the EGCE with the two proper scoring rule-based metrics. We start by ob-

serving that the proper scoring rule-based metrics behave in a symmetrical way, meaning that adding high-confidence

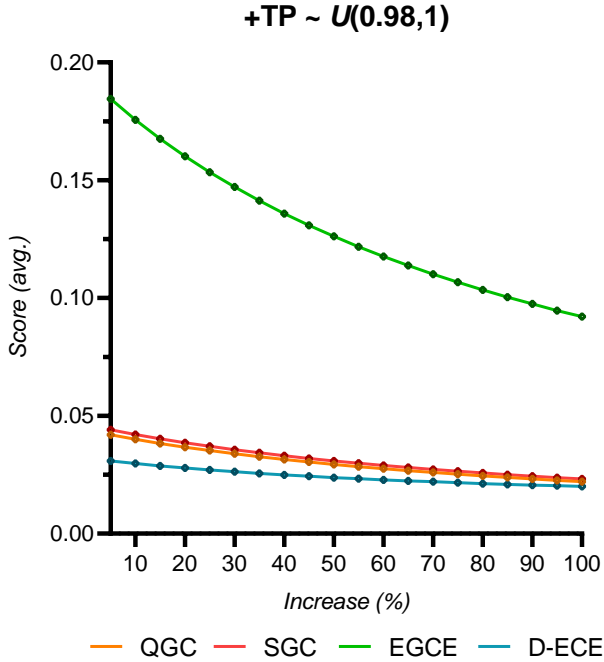


Fig. 5: Evaluating QGC score, SGC score, EGCE and D-ECE, with increasing proportions of True Positive detections, with confidence scores extracted from a Uniform distribution in the interval $[0.98,1]$.

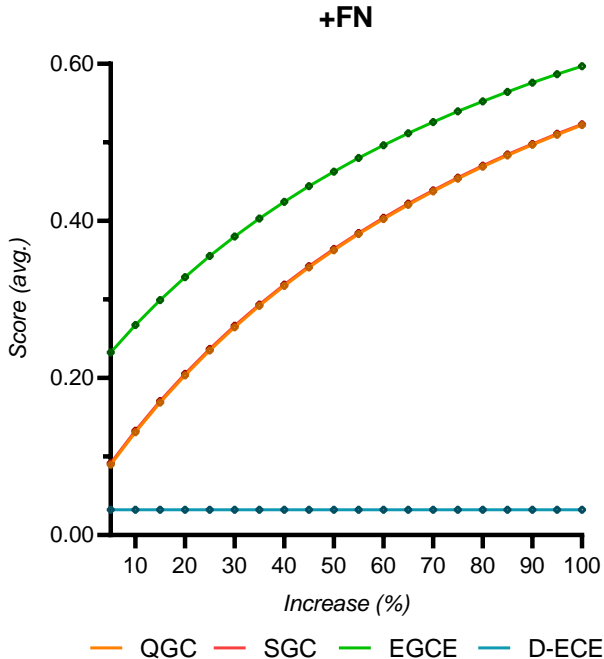


Fig. 6: Evaluating QGC score, SGC score, EGCE and D-ECE, with increasing proportions of False Negative detections.

False Positives produces the same negative effect as adding low-confidence True Positives (comparing Figures 1 and 2), just like adding high-confidence True Positives produces the

same positive effect as adding low-confidence False Positives (comparing Figures 4 and 3). Contrarily, the EGCE penalizes high-confidence False Negatives more than low-confidence True Positives, as well as rewards high-confidence True Positives more favorably than low-confidence False Positives. This behaviour can be advantageous since it is more consistent with a general evaluation of an object detection model (that will obviously favour True Positive detections over the False Positive counterparts).

Finally, we compare the behaviour of the three uncertainty calibration metrics proposed in this work (QGC score, SGC score and EGCE) with D-ECE. As previously referred, the D-ECE can be interpreted through our theoretical formulation as *local calibration* metric (in contrast to *global calibration* metrics); therefore, as illustrated in Figure 6, the D-ECE is completely not sensible to False Negatives, while the other three metrics show a relatively strong decrease in performance when exposed to high proportions of False Negatives. Furthermore, contrarily to the other metrics, the D-ECE still has small increases in values when exposed to a larger proportion of supposedly “desirable” detections (*i.e.*, high-confidence True Positives and low-confidence False Positives); only in the edge case presented in Figure 5 we witness a slight decrease in D-ECE.

On a final note, we observe that it is expectable that the EGCE is capable of having a more sensitive behaviour in cases like those represented in Figures 4 and 5, since the other three metrics start already with a relatively low score.

VII. FINAL REMARKS

The present work introduces a comprehensive theoretical and practical framework for assessing uncertainty calibration in object detection. The evaluation metrics proposed in the context of such framework are successfully used to evaluate the calibration of uncertainty estimates in a practical object detection scenarios. From the empirical evaluation of such metrics, some important conclusions can be derived:

- Contrarily to the D-ECE, the three proposed evaluation metrics (QGC score, SGC score and EGCE) show robust sensitivity in the presence of False Negatives.
- The QGC score and the SGC score show similar behaviour, with the SGC being slightly more sensitive to increasing proportions of “undesirable” predictions. As such, choosing between only one of these metrics seems to be reasonable.
- The EGCE, contrarily to both the QGC score and the SGC score, does not have a symmetrical behaviour towards True Positives and False Positives, and also shows higher sensibility with increasing proportions of “desirable” predictions, than the latter referred metrics. As such it is useful to use both EGCE and a proper scoring rule-based metric, since they offer different perspectives to the evaluation of uncertainty calibration.
- Although shown to be less robust than the proposed metrics, the D-ECE can still be useful to strictly assess *local calibration* (instead of *global calibration*).

On a final note, although in our experiments the uncertainty calibration metrics are used considering a fixed IoU threshold

of 0.5, these metrics can be evaluated across different IoU thresholds, as is occasionally carried out with mAP evaluation.

REFERENCES

- [1] G. W. Brier et al. Verification of forecasts expressed in terms of probability. *Monthly weather review*, 78(1):1–3, 1950.
- [2] P. Conde and C. Prenebida. Adaptive-TTA: accuracy-consistent weighted test time augmentation method for the uncertainty calibration of deep learning classifiers. In *33rd British Machine Vision Conference 2022, BMVC 2022, London, UK, November 21-24, 2022*. BMVA Press, 2022.
- [3] T. Gneiting and A. E. Raftery. Strictly proper scoring rules, prediction, and estimation. *Journal of the American statistical Association*, 102(477):359–378, 2007.
- [4] C. Guo, G. Pleiss, Y. Sun, and K. Q. Weinberger. On calibration of modern neural networks. In *International Conference on Machine Learning (ICML)*, pages 1321–1330. PMLR, 2017.
- [5] G. Jocher, A. Chaurasia, A. Stoken, J. Borovec, NanoCode012, Y. Kwon, K. Michael, TaoXie, J. Fang, imyhxy, Lorna, Z. Yifu, C. Wong, A. V, D. Montes, Z. Wang, C. Fati, J. Nadar, Laughing, UnglvKitDe, V. Sonck, tkianai, yxNONG, P. Skalski, A. Hogan, D. Nair, M. Strobel, and M. Jain. ultralytics/yolov5: v7.0 - YOLOv5 SOTA Realtime Instance Segmentation, Nov. 2022.
- [6] F. Kuppers, J. Kronenberger, A. Shantia, and A. Haselhoff. Multivariate confidence calibration for object detection. In *Proceedings of the IEEE/CVF Conference on Computer Vision and Pattern Recognition Workshops*, pages 326–327, 2020.
- [7] T. Lin, M. Maire, S. J. Belongie, L. D. Bourdev, R. B. Girshick, J. Hays, P. Perona, D. Ramanan, P. Dollár, and C. L. Zitnick. Microsoft COCO: common objects in context. *CoRR*, abs/1405.0312, 2014.
- [8] J. Moon, J. Kim, Y. Shin, and S. Hwang. Confidence-aware learning for deep neural networks. In *International Conference on Machine Learning (ICML)*, pages 7034–7044. PMLR, 2020.
- [9] M. A. Munir, M. H. Khan, S. Khan, and F. S. Khan. Bridging precision and confidence: A train-time loss for calibrating object detection. In *Proceedings of the IEEE/CVF Conference on Computer Vision and Pattern Recognition*, pages 11474–11483, 2023.
- [10] M. A. Munir, M. H. Khan, M. Sarfraz, and M. Ali. Towards improving calibration in object detection under domain shift. *Advances in Neural Information Processing Systems*, 35:38706–38718, 2022.
- [11] M. P. Naeni, G. Cooper, and M. Hauskrecht. Obtaining well calibrated probabilities using bayesian binning. In *Twenty-Ninth AAAI Conference on Artificial Intelligence*, 2015.
- [12] J. Nixon, M. W. Dusenberry, L. Zhang, G. Jerfel, and D. Tran. Measuring calibration in deep learning. In *CVPR Workshops*, volume 2, 2019.
- [13] Y. Ovadia, E. Fertig, J. Ren, Z. Nado, D. Sculley, S. Nowozin, J. Dillon, B. Lakshminarayanan, and J. Snoek. Can you trust your model’s uncertainty? evaluating predictive uncertainty under dataset shift. *Advances in Neural Information Processing Systems (NeurIPS)*, 32, 2019.
- [14] B. Pathiraja, M. Gunawardhana, and M. H. Khan. Multiclass confidence and localization calibration for object detection. In *Proceedings of the IEEE/CVF Conference on Computer Vision and Pattern Recognition*, pages 19734–19743, 2023.
- [15] J. Tian, D. Yung, Y.-C. Hsu, and Z. Kira. A geometric perspective towards neural calibration via sensitivity decomposition. *Advances in Neural Information Processing Systems (NeurIPS)*, 34:26358–26369, 2021.
- [16] D. Widmann, F. Lindsten, and D. Zachariah. Calibration tests in multi-class classification: A unifying framework. *Advances in Neural Information Processing Systems (NeurIPS)*, 32, 2019.